Journal of Membrane Science & Research

journal homepage: www.msrjournal.com

Research Paper

A Greener Procedure to Prepare TiO_2 Membranes for Photocatalytic Water Treatment Applications

Izumi Kumakiri *, Kohei Murasaki, Shotaro Yamada, Azzah Nazihah Binti Che Abdul Rahim, Haruyuki Ishii

Graduate School of Sciences and Technology for Innovation, Faculty of Engineering, Yamaguchi University, 2-16-1 Tokiwadai Ube, 755-8611 Japan

Article info

Received 2022-02-27
Revised 2022-05-27
Accepted 2022-05-27
Available online 2022-05-27

Keywords

Formic acid
Photocatalytic oxidation
Silver
Titanium dioxide membrane
Water treatment

Highlights

- TiO_2-ceramic membranes were prepared using commercial TiO_2 powder (P25, Evonik)
- Solvent-free dry deposition followed by heating and low-temperature wet deposition were compared
- Silver was photo-chemically deposited onto the TiO_2 membranes
- Formic acid decomposition rate was depending on the preparation method of TiO_2 membranes

Graphical abstract

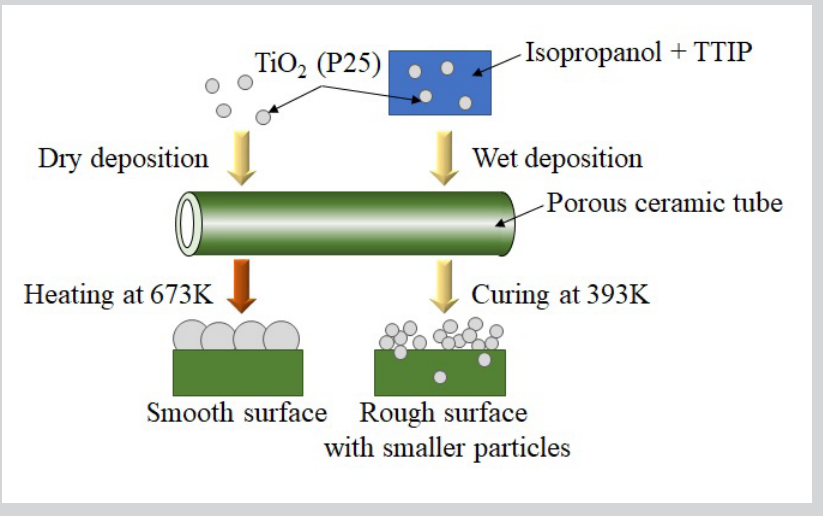

Abstract

A commercial titanium dioxide powder (TiO_2, P25, Evonik) was immobilized on porous mullite tubes by simple mechanical scrubbing followed by heat treatment at 673 K in air and by dip-coating followed by curing at 393K in air. A dispersant of P25 powder in isopropyl alcohol with a small amount of titanium isopropoxide (TIPP) was used for dip-coating. The surface morphology of TiO_2 membranes was different depending on the preparation method: mechanical scrubbing resulted in a smoother surface and dip-coating resulted in a rougher surface consisting of particles smaller than 0.1 μm, which size is almost the same as P25. TiO_2 and Ag-TiO_2 membranes were tested with formic acid decomposition in water. The difference in morphology influenced the photochemical deposition of silver on the TiO_2 membranes. Silver deposition improved the formic acid decomposition rate of TiO_2 membranes prepared by mechanical scrubbing. This decomposition rate decreased when silver was deposited on TiO_2 membranes prepared by dip-coating.

1. Introduction

The variety of chemicals discharged from factories is increasing as the industry creates new types of products. Poorly bio-degradable chemicals in wastewater remain in the environment for a long time. Some of such persistent organic pollutants (POPs) are suspected to pose a health risk even in dilute concentrations [1]. For example, polyfluoroalkyl substances (PFAS) are used in coatings, firefighting forms, and other products [2]. Among PFAS, perfluorooctanesulfonate (PFOS) and perfluorooctanate (PFOA) are recognized as persistent, bioaccumulative, and with possible health risk chemicals even in ppb or ppm orders [3]. New water cleaning technologies are required to treat these dilute but persistent chemicals.

Photocatalysis with semiconductors is one way to treat dilute but poorly biodegradable organic pollutants in water [4,5]. The process is simple as it does not require any additional chemicals and can decompose pollutants at ambient temperature and pressure. Titania dioxide (TiO_2) and TiO_2-based materials are the most studied semiconductors for such applications as they are robust and cost-effective [6]. Various modifications have also been proposed to make TiO_2 active under visible light [7]. Visible light-driven water treatment is attractive especially for places with unreliable electricity supply due to an insufficient facility or under natural hazard conditions.

The applications of semiconductors for water treatment are performed often by dispersing powder materials in contaminated water. Immobilizing

* Corresponding author: izumi.k@yamaguchi-u.ac.jp (I. Kumakiri)

DOI: 10.22079/JMSR.2022.549416.1535

these powder catalysts on a membrane will make the water treatment process simpler as a separation of catalysts from treated water is not required. While photo-catalytic membranes have less surface area than a powder dispersed system which reduces the performance [8], membrane configurations can add extra functions. For example, if TiO_2 membranes are applied as membrane filtration, some contaminants are rejected by the pores of the membrane, and others are decomposed while permeating through the membrane [9]. Photocatalysts fixed on membranes reduce the fouling influence by decomposing pollutants clogging the pores [10]. It can also enhance the hydrophilicity of the membrane that results in the higher water flux through the membrane [11]. Alternatively, membranes can be used as a contractor. In this configuration, water flows over the catalytic membrane surface and oxygen, which is required to decompose dissolved pollutants by catalytic oxidation, is supplied through a porous membrane. As water flows along the membrane surface, fouling is reduced in this configuration. In addition, the facilitated oxygen supply to the photocatalysts in the contactor configuration was reported to improve the reaction kinetics [12].

TiO_2 membranes have been prepared by different methods. Typical conditions are listed in Table 1. The sol-gel method is a common procedure to form a thin mesoporous TiO_2 layer on porous ceramic support [9,13,14]. Various techniques, such as chemical vapor deposition (CVD) [15], anodization of Ti foil to form TiO_2 nanotubes [16], and hydro/solvothermal syntheses are also reported to synthesize TiO_2-ceramic composite membranes. Details can be found in several review papers [17]. In these cases, titanium precursors, such as titanium isopropoxide (TIPP), are often used as a starting material followed by heat treatment typically over 737K. The preparation conditions affect the microstructure and crystalline phases of TiO_2 and change the catalytic performance [18].

Alternatively, powder TiO_2 can be shaped as a membrane. In this way, powder catalysts with known performance, such as commercial P25 (EVONIC Industries, Germany) being used as a benchmark of photo-catalyst [19], can be employed. Membranes are shaped by dispersing powder in a polymer matrix and forming polymer-TiO_2 films [20,21] or by sintering the powder on support. Binder-less immobilization is also possible by e.g. calcining a porous ceramics support coated with TiO_2 powder at 673K [12]. Low-temperature synthesis is investigated especially for the production of dye-sensitized solar cells to use polymeric film as support. However, lowering the calcination temperature reduces the sintering degree. Accordingly, it results in poorly jointed TiO_2 powder and fragile TiO_2 membranes. Adding a small amount of inorganic binders, such as TIPP and $Ca(OH)_2$, enhances the adhesion between TiO_2 powders and between TiO_2 and support even with curing at low temperatures e.g. 393K [22,23]. The low-temperature TiO_2 membrane preparation is attractive as it does not require expensive facilities. Application of this method to form a TiO_2 layer on a porous tubular support is limited and the membrane stabilities are not well-known. In addition, the binders may hinder the photocatalytic activity of the TiO_2 powder by covering its surface.

In this study, we compared TiO_2 membranes prepared by immobilizing P25 powder on porous ceramic tubes by different methods. Binder-less immobilization by heating at 673K, dip-coating using a dispersant of P25 in isopropanol with TIPP as an inorganic binder, and a combination of these two methods were used. Deposition of metals is reported to enhance the photocatalytic activity of TiO_2 [24,25]. In this study, silver was photochemically deposited into TiO_2 membranes prepared by different methods. The photocatalytic performance of these membranes was evaluated by formic acid decomposition in water.

2. Material and methods

2.1. Materials

Mullite porous tubes (NIKKATO Corporation, Japan, mean pore size 1.3μm, porosity 42%, o.d. 12mm, i.d. 9mm, length 100 mm) were used as supports. P25 (EVONIC Industries, Germany) was used as TiO_2 powder. Titanium tetra-iso-propoxide (TTIP, FUJIFILM Wako Pure Chemical Corporation, Japan, purity 95%) was used as a binder of P25. Isopropanol (IPA, FUJIFILM Wako Pure Chemical Corporation, Japan, purity ≥99.7%) was used as a dispersant of P25. Silver acetate (CH_3COOAg, FUJIFILM Wako Pure Chemical Corporation, Japan, purity 97%) was used as a silver source. P25 was provided from EVONIC Industries. Other materials were purchased.

2.2. Powder and membrane preparations

P25 powder was mechanically scrubbed onto the outer surface of mullite tubes. Then, coated membranes were heated at 673K for three hours in the air. A ramp rate of 10 K/min was used for the heating and the furnace was naturally cooled down to the room temperature. After heating, membranes were washed with water to remove any loosely attached powder and dried at 353K in an air-drying oven.

Dip-coating was used as another method of applying P25 on the supports. First P25 powder was dispersed in IPA solution and ultra-sonification was applied for 30 minutes. Then, TTIP solution was added dropwise under stirring until the molar ratio of TTIP to P25 became 0.1: 1. Mullite supports and mechanically P25-coated mullite supports were dipped into the solution, dried in the air, then heated at 393 K for one hour. After cooled down to room temperature, membranes were washed with water and dried overnight at room temperature and then 353K in an air-drying oven.

Silver was deposited by photo-reduction onto some of the TiO_2 membranes. Similar conditions as described in the previous study [26] were used. First, a membrane was soaked into $1x10^{-5}$ mol/L silver acetate solution and the light was irradiated for 1.5 hours. Black lamps (11 μW/cm^2, λmax = 352 nm, FL8BLB, Toshiba Co., Japan) were used as the light source. The change of Ag concentration in the solution was measured by inductivity coupled plasma (ICP, SPS3500, SII nanotechnology co., Japan).

Table 1
TiO_2-ceramic composite membrane preparation examples

TiO_2 layer preparation conditions				Photocatalytic performance tests		Ref.
Method	**Raw materials**	**Support**	**Heat treatment conditions**	**Pollutants**	**Conditions**	
Sol-Gel / Dip coating	1 TTIP* : 14 isopropanol : 4 H_2O : 0.4 HCl	α-Alumina tube (pore size 1 μm)	Calcination at 723 K	Trichloroethylene and polyethyleneimine	4W Black light lamp (peak 350 nm)	[9]
Sol-Gel / Dip coating	1 TTIP* : 45 isopropanol : 6 acetic acid : 1 Tween 80**	Glass plate and alumina disk (pore size 0.1 μm)	Calcination at 737 K for 15 minutes	3.0 mM methylene blue and 0.2 mM Creatinine in water	15W mercury lamp (peak 365 nm, 3.48 mW/cm^2)	[14]
CVD	TTIP* vapor with N_2 sweep	Vycor glass tube (pore size 4 nm)	473-673 K, 1 atm,	-	-	[15]
Anodization + annealing	Ti foil	Placed on a glass plate with TiO_2 sol	Annealing at 573-1173 K for 2 hours	5 mg/L Rhodamine B in water	300 W UV lamp (peak 365 nm)	[16]
Doctor blade (Polymer-TiO_2 composite)	P25† dispersed in polyethylene oxide and polyethylene glycol	Glass plate	673 K for 3hours	Disinfection test with E. Coli	20W Black light lamp (ca. 1 mW/cm^2)	[20]
Spin coating (Polymer-TiO_2 composite)	Commercial TiO_2 powder dispersed in poly vinyl alcohol	Alumina flat sheet	1073 K for 3hours	5 mg/L humic acid in water	UV lamp (peak 365 nm, 2.5 mW/cm^2)	[21]
Mechanical scrubbing / Dip-coating	P25 † with/without TTIP*	Mullite tube (pore size 1.3 μm)	Calcination at 673 K or at 393 K	240 mg/L formic acid in water	0.8W Black light lamp (peak 352 nm, 11 μW/cm^2)	This study

*TTIP: Titanium tetraisopropoxide ($Ti[OCH(CH_3)_2]_4$), **Tween 80: Polyoxyethylenesorbitan monooleate, † P25: Commercial TiO_2 powder (EVONIC Industries, Germany)

2.3. Characterization

Powder samples were analyzed by transmission electron microscopy (TEM, JEM-2100, JEOL Ltd., Japan) and X-ray diffraction (XRD, XRD-6100, SHIMADZU Co., Japan) with Cu-Kα radiation. The TEM sample was prepared by dispersing the powder sample in ethanol with ultrasonication and drop-casting the suspension to the TEM grid (Cu200J, JEOL, Tokyo, Japan). The specific surface area (BET) was calculated from an N_2 adsorption isotherm, measured with a BELSORP MAX G instrument (MicrotracBEL Corp., Osaka, Japan). The adsorption of N_2 was measured at the temperature of liquid nitrogen (77K). Before measuring, all of the samples were degassed at 393 K for 3 hours. Membranes were characterized by XRD and scanning electron microscopy (FE-SEM, JSM-6335F, JSM-7600F, JEOL Ltd., Japan).

Membrane performance was investigated by the oxidation rate of formic acid in water. Fig. 1 shows a schematic view of a rig. As a light source, 4 pieces of UV (black lamps, 11 μW/cm^2, λmax = 352 nm, FL8BLB, Toshiba Co., Japan) were placed as shown in the figure. Oxygen was supplied as bubbles at a flow rate of 20 mL/min. All the experiments were performed at room temperature.

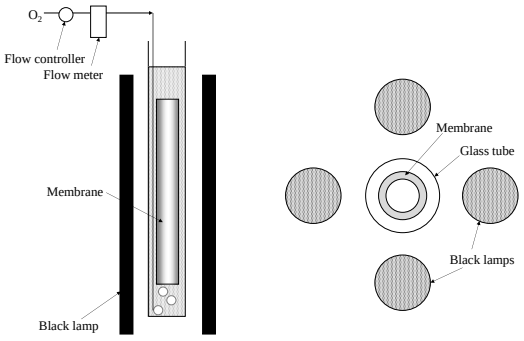

Fig. 1. Schematic view of a photocatalytic membrane test unit (left: side view, right; top view)

3. Results and Discussion

3.1. P25-TTIP composite material

TTIP solution formed white powder by reacting with humidity in the air [27]. The following equations show examples of the hydrolysis and the condensation reactions.

$$Ti(OCH(CH_3)_2)_4 + 2H_2O \rightarrow Ti(OCH(CH_3)_2)_3OH + C_3H_8O$$
$$2Ti(OCH(CH_3)_2)_3OH \rightarrow Ti(OCH(CH_3)_2)_3OTi(OCH(CH_3)_2)_3 + H_2O$$

The obtained powder was amorphous as analyzed by XRD (Fig. 2, the sample indicated as TTIP-RT). Heating the powder at 393 K for one hour did not change the XRD pattern and the powder remained amorphous. On the contrary, after heating the powder at 673 and 873 K in the air for three hours, the amorphous phase changed to crystalline as shown in the figure. The main peaks corresponded to anatase and rutile after heat treating the powder at 673 and 873 K, respectively.

P25 powder was dispersed in isopropanol, then 10 mol% of TTIP to TiO_2 was added. Drying the dispersant at room temperature formed white powder. Then the powder was heated at 393K for one hour (the sample is named P25-TTIP-393K). Fig. 3a shows the XRD patterns of the sample. No significant difference was observed in the XRD patterns compared with P25 powder. No trace of amorphous phase was found in the P25- TTIP -393K sample, for the amount of amorphous phase formed by the hydrolysis and condensation of TTIP was small. Fig.s 3 b and c show the morphologies of pristine P25 and TTIP modified P25 (P25-TTIP-393K) powders, respectively. While XRD peaks were the same with these powders, TEM analyses revealed the existence of some amorphous material in between P25 particles as shown in Fig. 3b. Such an amorphous phase was not observed in the original P25 powder. As reported by H. Kim et al., TTIP seemed to be working as an inorganic binder of P25 particles [23]. A large part of the TiO_2 surface was not covered by amorphous material from the TEM observations. Fig. 3d shows the N_2 isotherms. The BET surface areas of P25 and P25-TTIP-393K were 50 and 57 m^2/g, respectively. The pore size distribution with BJH analysis showed some mesopores in the P25-TTIP composite powder (Fig. 3e). Even though P25 particles were partially covered by the amorphous material originating from TTIP, the amorphous layer is porous and expected to allow the access of reactants to the P25 surface.

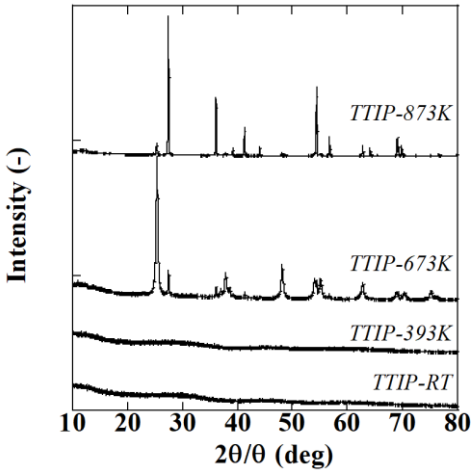

Fig. 2. XRD of powder samples prepared from TTIP at different temperature (TTIP-RT: dried at room temperature, TTIP-393K, 673K, 873K: TTIP-RT powder dried at indicated temperature)

3.2. TiO_2 membranes prepared by immobilizing P25 particles

The tubular supports were not polished after purchasing. Accordingly, the support surface was rather rough and had pores of a few micron maters as shown in Fig. 4a. After applying TiO_2 particles by different methods, the support surface was completely covered with TiO_2 particles but the morphologies were different from the deposition method. Fig.s 4b and c show the surface of a membrane prepared by dip-coating in different magnifications. The membrane had many cracks as shown in Fig. 4b. Agglomeration of particles during the drying step of membranes after dip-coating may have caused these defects. The particles at the surface of the membrane were less than 0.1μm, which size and shape were similar to the commercial P25. As the membranes were treated with a low curing temperature of 393K, P25 kept its morphology. The thickness of the TiO_2 layer was about a few micrometers as observed by a cross-sectional view of the membrane by SEM. Some TiO_2 particles were found inside the porous support in addition to the surface. This is because the support average pore size was 1.3 μm, which is large enough to penetrate TiO_2 particles having a particle size less than 0.1 μm [28].

On the contrary, the membrane surface after mechanical deposition of P25 powder followed by calcination at 673K was smooth as shown in Fig. 4d. The particle size at the surface of the membrane was about 100 to 300 nm and larger than the size of P25, showing some degree of sintering during the calcination. No change in the TiO_2 phase before and after the calcination was observed by XRD. The major phase was maintained as anatase, for the calcination temperature was lower than the phase transition temperature to rutile. By this dry method, about 160±0.7 mg/cm^2 of P25 was fixed on the support. The standard error was calculated with the results of 21 samples. Repeating the mechanical scrubbing did not increase the deposition of P25 particles by more than 50mg/cm^2. On the contrary, applying dip-coating to the membranes prepared by mechanical scrubbing increased the amount of the deposits by about 230±5 mg/cm^2. TTIP in the dip-coating solution may help the deposition of P25 powder to the membrane. The standard error was calculated from 9 samples. When dip-coating was applied directly to the mullite support, the deposition was about 150±2 mg/cm^2. A larger amount of P25 can be deposited on the tubular support by a combination of dry application and dip-coating.

Photocatalytic activity of formed TiO_2 membranes was studied by decomposing formic acid in water under UV light irradiation (λmax = 352 nm). Fig. 5 shows the change of formic acid concentration as a function of time. Concentration decreased linearly with time. Zero-order assumption fits well the data as reported earlier for the oxidation of formic acid in water [29,30]. The lines in the figure show the concentration change with a zero-order equation using the rate constant (k) in Table 2. Kinetic data obtained with membranes prepared under the same conditions had some deviation but can be fitted with a rate constant ± 10% to the value listed in the table. Half time ($t_{0.5}$), the time required to achieve a 50% reduction in the concentration from the initial concentration, estimated from the zero-order fitting is also shown in the table.

A TiO_2 membrane made by applying dip-coating directly to the mullite support showed the slowest oxidation rate even though the membrane deposited a similar amount of TiO_2 to the membranes prepared by mechanical scrubbing. This was due to some parts of the TiO_2 powder being located inside the porous support as observed by SEM, where light does not penetrate. Employing supports with a smaller pore size will avoid such penetration. Asymmetric

ceramic supports with a pore size of e.g. 0.1 μm are commercially available, however, the price is one order higher than the cost of symmetric supports used in this study.

The fastest oxidation rate was obtained with membranes prepared by a combination of mechanical scrubbing and dip-coating. The results of three membranes prepared under the same conditions are shown in the figure. The halftime of membranes prepared by mechanical scrubbing was about 21 minutes. On the contrary, applying dip-coating after mechanical scrubbing improved the decomposition rate and the halftime got shorter to 17 minutes. The improvement in the rate constant was about 1.2 times, on the contrary, the total TiO_2 mass fixed on the membrane was 50% larger. The smaller size of TiO_2 particles at the surface of the membranes was expected to improve the decomposition rate. The miner enhancement observed may be due to the shading of particles in the membrane and light was not irradiating all the particle surface evenly. In addition, the binder may reduce the light intensity or hinder the diffusion of reactants to the TiO_2 surface even though they are porous. Light strength may be another limitation but due to the space limitation to install extra bulbs, strengthening the light intensity was not examined in this study.

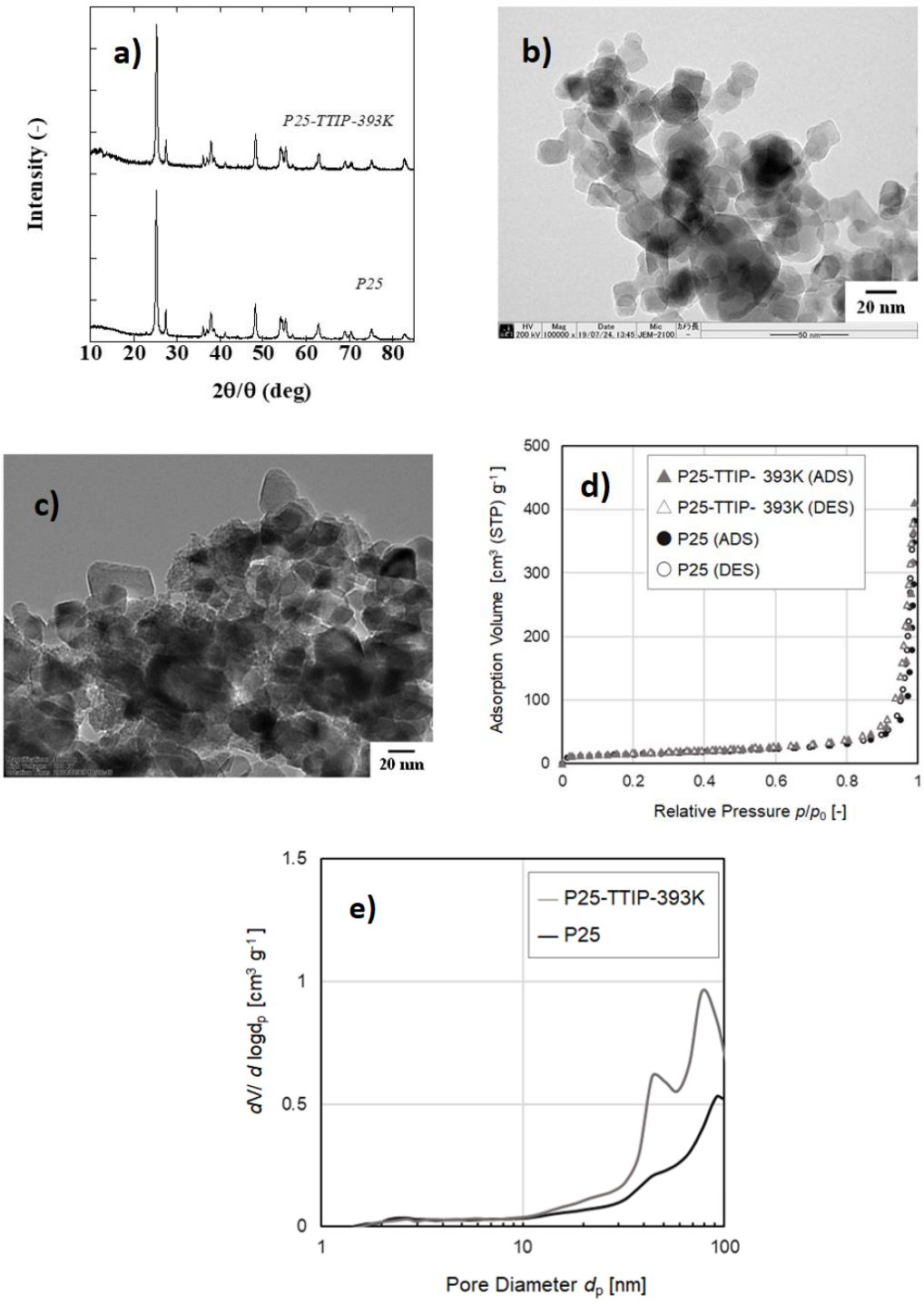

Fig. 3. Properties of P25 and P25-TTIP-393K composite powder (a) XRD of P25 powder (bottom) and P25-TTIP-393K composite powder cured at 393K, b) TEM image of P25 powder, c) TEM image of P25-TTIP composite powder cured at 393K, d) N_2 adsorption/desorption isotherms of P25 (○), P25-TTIP-393K composite powder(Δ), e) BJH pore-size distribution)

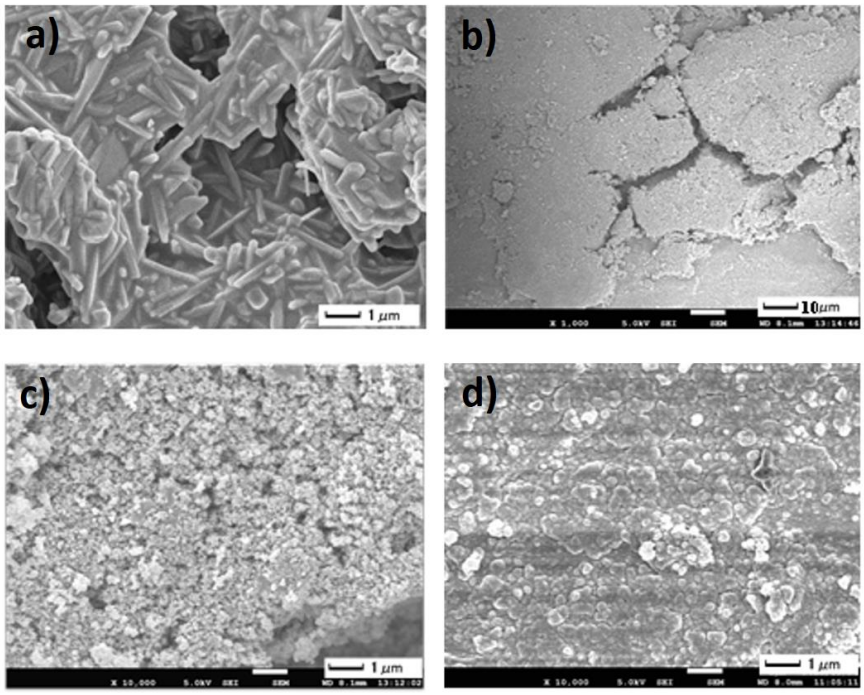

Fig. 4. Membrane surface views (a) Mullite support, b), c) TiO_2 membrane made by dip-coating and curing at 393K, d) TiO_2 membrane made by mechanical scrubbing followed by heating at 673 K)

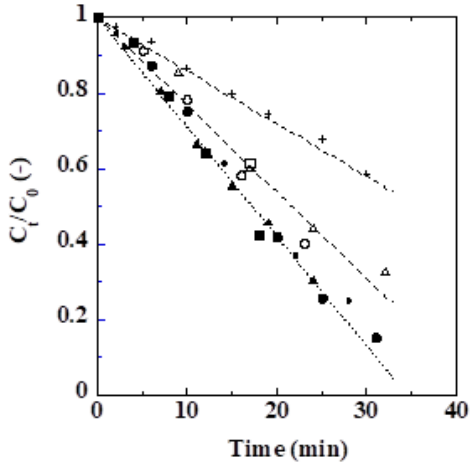

Fig. 5. Normalized formic acid concentration as a function of time (+: TiO_2 membranes prepared by dip coating, open keys: TiO_2 membranes prepared by mechanical scrubbing, closed keys: TiO_2 membranes prepared by mechanical scrubbing and dip-coating)

Table 2
Comparison of TiO_2 membranes prepared on porous mullite support

TiO_2 membrane preparation method	Amount of deposition (mg cm^{-2})	K-value (min^{-1})	$t_{0.5}$ (min)
Mechanical scrubbing	160±0.7	0.024	21
Mechanical scrubbing followed by dip-coating after	230±5	0.029	17
Dip-coating	150±2	0.014	36

3.3. Ag-TiO_2 membranes prepared by photoreduction

Silver was deposited on the TiO_2 membranes prepared by different methods by photo-reduction using a dilute silver acetate solution [26]. The concentration of silver in the solution decreased by about 90% after the photo-reduction analyzed by ICP for all the cases. The total amount of deposited silver was about 0.4 mol/m^2. The molar ratio between Ag and TiO_2 was about 20 ppm with a TiO_2 membrane prepared by mechanical scrubbing. This ratio was about 14 ppm with a membrane prepared by mechanical scrubbing and dip-coating. No silver was detected by XRD, probably because of its low amount and small size.

The color of the Ag-TiO_2 membranes was different from how the TiO_2 layer was prepared. The TiO_2 membranes were white and the color changed to red-brown for membranes prepared by mechanical scrubbing and yellow-blue for membranes prepared by dip-coating after mechanical scrubbing. The color of the Ag-TiO_2 membranes became white after keeping the membranes in the room for a few days. This was probably due to the change of deposited silver to colorless silver ion by reacting with oxygen in the air under visible light [31]. Membranes got back to color when soaked them into a formic acid solution and UV light was applied. Examples are shown in Fig. 6. The difference in the color of Ag-TiO_2 membranes was due to the differences in the size and the shape of the silver particle [32,33]. For example, the color became redder with increasing the size of silver particles [34]. TiO_2 membranes prepared by dip-coating after mechanical scrubbing showed the fastest decomposition of formic acid as shown in Fig. 5, which indicated a larger photo-active TiO_2 surface area compared to TiO_2 membranes prepared by mechanical scrubbing. As the photo-reduction sites for silver deposition were larger with the dip-coated membrane, silver may be deposited as smaller particles.

While the total amount of silver was almost the same, the influence of silver deposition on formic acid decomposition was different from how the TiO_2 membranes were prepared as shown in Fig. 7. Formic acid oxidation rate showed a small increase by silver deposition on a TiO_2 membrane prepared by mechanical scrubbing (Fig. 7a). On the contrary, the silver deposition showed a negative influence on TiO_2 membranes prepared by dip-coating after mechanical scrubbing (Fig. 7b). Two membranes prepared under the same conditions showed the same trend as shown in the figure.

Metal deposition to TiO_2 can improve the photocatalytic activity but the deposition amount has an optimum value. For example, Sclafani *et al.* applied Ag-TiO_2 powder prepared by photo-deposition to 2-propanol oxidation and reported about 1 wt% silver deposition improved the oxidation rate [24]. They also reported that excess silver than the optimum amount reduced the kinetics. A similar tendency was reported by Sobana *et al.* with azo dye Direct RED degradation [35], by Shchukin *et al.* with 2-chlorophenol [36], and by Shokri *et al.* with chloramphenicol decomposition [37] in water. The optimum metal amount varies to the conditions but is often reported to be about 1 wt% [24,37] but sometimes less than 0.02 wt% [25,36] to the TiO_2 mass. The reason for the enhanced photocatalytic activity by adding a small amount of metal was explained by the improved charge separation induced by light [24,37]. The negative influence of metal addition was suspected to be caused by the increase of hole capture probability [24,37], by shading the light irradiation [37], and by the agglomeration of metal particles that decreases the adsorption of pollutants [38]. Tiny silver particles are reported to increase the recombination rate of holes and electrons [36], which may be the situation with Ag-TiO_2 membranes prepared after dip-coating and the reason for the decreased decomposition rate.

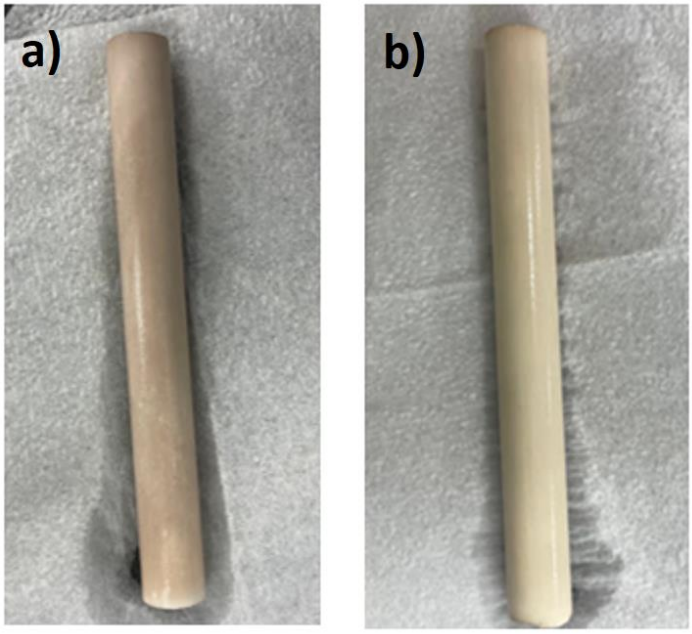

Fig. 6. Ag-TiO_2 membranes after decomposing formic acid in water (a): the base TiO_2 membrane was made by mechanical scrubbing, b): the base TiO_2 membrane was made by dip-coating after mechanical scrubbing)

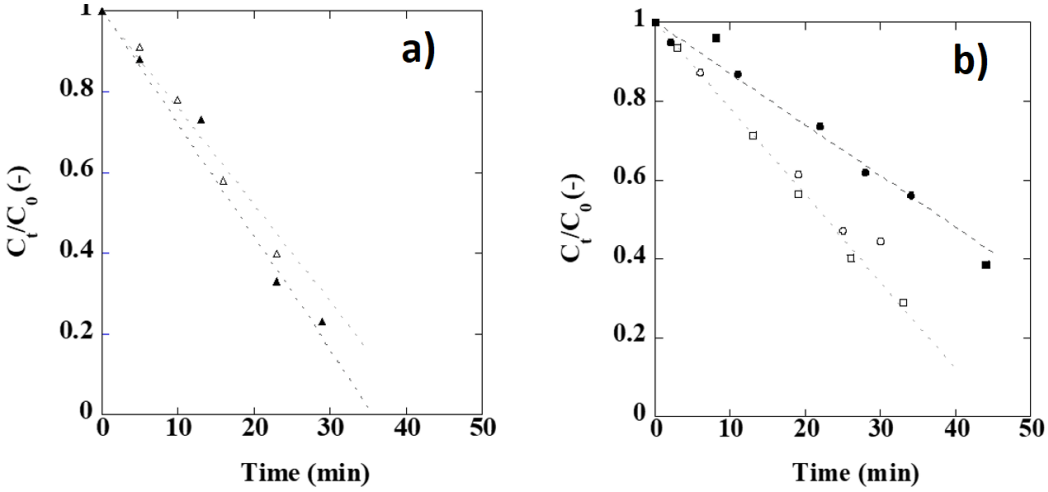

Fig. 7. Normalized formic acid concentration in the solution as a function of time (a) Δ: original TiO_2 membrane formed by mechanical scrubbing, ▲: Ag-TiO_2 membrane by photochemically depositing Ag on Δ; b) ○, □: original TiO_2 membranes formed by mechanical scrubbing and dip-coating, ●, ■: Ag-TiO_2 membrane by photochemically depositing Ag on ○, □)

4. Conclusions

TiO_2 membranes were prepared by applying commercial TiO_2 powder (P25, Evonik) on the outer surface of porous ceramic tubes. TiO_2 particles were immobilized by heating at 673K after mechanically scrubbing the particles to the support. This method did not require any solvent or binder and resulted in a smoother surface as a result of partial sintering. Applying dip-coating using a dispersant containing P25 particles in isopropanol and low-temperature curing prevented the enlargement of TiO_2 particles. TTIP added to the dispersant acted as an inorganic binder and fixed TiO_2 particles to the membrane.

The influence of silver deposition to TiO_2 membranes on photocatalytic activity depended on how the TiO_2 membranes were prepared. The larger surface area of TiO_2 membranes prepared by dip-coating made the silver particle size smaller, which may have increased the recombination of holes and electrons, and reduced the photocatalytic activity.

Acknowledgments

This work was supported by JST SICORP Grant Number JPMJSC18C5, Japan.

References

[1] K.S. Ritter, Paul Sibley, Ken Hall, Patricia Keen, Gevan Mattu, Beth Linton, Len. Sources, pathways, and relative risks of contaminants in surface water and groundwater: a perspective prepared for the Walkerton inquiry. Journal of Toxicology and Environmental Health Part A 65 (2002) 1-142 https://doi.org/10.1080/152873902753338572

[2] J. Glüge; M. Scheringer; I.T. Cousins; J.C. DeWitt; G. Goldenman; D. Herzke; R. Lohmann; C.A. Ng; X. Trier; Z. Wang. An overview of the uses of per-and polyfluoroalkyl substances (PFAS). Environmental Science: Processes & Impacts 22 (2020) 2345-2373 10.1039/D0EM00291G

[3] F. Suja; B.K. Pramanik; S.M. Zain. Contamination, bioaccumulation and toxic effects of perfluorinated chemicals (PFCs) in the water environment: a review paper. Water Science and Technology 60 (2009) 1533-1544 https://doi.org/10.2166/wst.2009.504

[4] M. Trojanowicz; A. Bojanowska-Czajka; I. Bartosiewicz; K. Kulisa. Advanced oxidation/reduction processes treatment for aqueous perfluorooctanoate (PFOA) and perfluorooctanesulfonate (PFOS)–a review of recent advances. Chemical Engineering Journal 336 (2018) 170-199 https://doi.org/10.1016/j.cej.2017.10.153

[5] A.A. Yaqoob; T. Parveen; K. Umar; M.N. Mohamad Ibrahim. Role of nanomaterials in the treatment of wastewater: a review. Water 12 (2020)

495 https://doi.org/10.3390/w12020495
[6] I. Gehrke; A. Geiser; A. Somborn-Schulz. Innovations in nanotechnology for water treatment. Nanotechnology, science, and applications 8 (2015) 1 . 10.2147/NSA.S43773
[7] K. Wetchakun; N. Wetchakun; S. Sakulsermsuk. An overview of solar/visible-light-driven heterogeneous photocatalysis for water purification: TiO2-and ZnO-based photocatalysts used in suspension photoreactors. Journal of industrial and engineering chemistry 71 (2019) 19-49 https://doi.org/10.1016/j.jiec.2018.11.025
[8] C.M. Ling; A.R. Mohamed; S. Bhatia. Performance of photocatalytic reactors using immobilized TiO2 film for the degradation of phenol and methylene blue dye present in water stream. Chemosphere 57 (2004) 547-554 https://doi.org/10.1016/j.chemosphere.2004.07.011
[9] T. Tsuru; T. Toyosada; T. Yoshioka; M. Asaeda. Photocatalytic reactions in a filtration system through porous titanium dioxide membranes. Journal of chemical engineering of Japan 34 (2001) 844-847 https://doi.org/10.1252/jcej.34.844
[10] P. Gao; Z. Liu; M. Tai; D.D. Sun; W. Ng. Multifunctional graphene oxide–TiO2 microsphere hierarchical membrane for clean water production. Applied Catalysis B: Environmental 138 (2013) 17-25 https://doi.org/10.1016/j.apcatb.2013.01.014
[11] J.-P. Méricq; J. Mendret; S. Brosillon; C. Faur. High-performance PVDF-TiO2 membranes for water treatment. Chemical Engineering Science 123 (2015) 283-291 https://doi.org/10.1016/j.ces.2014.10.047
[12] I. Kumakiri; S. Diplas; C. Simon; P. Nowak. Photocatalytic membrane contactors for water treatment. Industrial & engineering chemistry research 50 (2011) 6000-6008 https://doi.org/10.1021/ie102470f
[13] T. Tsuru; M. Narita; R. Shinagawa; T. Yoshioka. Nanoporous titania membranes for permeation and filtration of organic solutions. Desalination 233 (2008) 1-9 https://doi.org/10.1016/j.desal.2007.09.021
[14] H. Choi; E. Stathatos; D.D. Dionysiou. Sol-gel preparation of mesoporous photocatalytic TiO2 films and TiO2/Al2O3 composite membranes for environmental applications. Applied Catalysis B: Environmental 63 (2006) 60-67 https://doi.org/10.1016/j.apcatb.2005.09.012
[15] H.Y. Ha; S.W. Nam; T.H. Lim; I.-H. Oh; S.-A. Hong. Properties of the TiO2 membranes prepared by CVD of titanium tetraisopropoxide. Journal of membrane science 111 (1996) 81-92 https://doi.org/10.1016/0376-7388(95)00278-2
[16] J. Liao; S. Lin; N. Pan; S. Li; X. Cao; Y. Cao. Fabrication and photocatalytic properties of free-standing TiO2 nanotube membranes with through-hole morphology. Materials characterization 66 (2012) 24-29. https://doi.org/10.1016/j.matchar.2012.02.005
[17] S. Leong; A. Razmjou; K. Wang; K. Hapgood; X. Zhang; H. Wang. TiO2-based photocatalytic membranes: A review. Journal of Membrane Science 472 (2014) 167-184 https://doi.org/10.1016/j.memsci.2014.08.016
[18] B.K. Mutuma; G.N. Shao; W.D. Kim; H.T. Kim. Sol-gel synthesis of mesoporous anatase–brookite and anatase–brookite–rutile TiO2 nanoparticles and their photocatalytic properties. Journal of colloid and interface science 442 (2015) 1-7 https://doi.org/10.1016/j.jcis.2014.11.060
[19] A. Wold. Photocatalytic properties of titanium dioxide (TiO2). Chemistry of Materials 5 (1993) 280-283 https://doi.org/10.1021/cm00027a008
[20] D.S. Kim; S.-Y. Kwak. Photocatalytic inactivation of E. coli with a mesoporous TiO2 coated film using the film adhesion method. Environmental science & technology 43 (2009) 148-151 https://doi.org/10.1021/es801029h
[21] L. Zhang; T.C.A. Ng; X. Liu; Q. Gu; Y. Pang; Z. Zhang; Z. Lyu; Z. He; H.Y. Ng; J. Wang. Hydrogenated TiO2 membrane with photocatalytically enhanced anti-fouling for ultrafiltration of surface water. Applied Catalysis B: Environmental 264 (2020) 118528. https://doi.org/10.1016/j.apcatb.2019.118528
[22] J. Chen; J. Luo; X. Jin; Y. Liu; J. Sun; L. Gao. Promotion of charge transport in low-temperature fabricated TiO2 electrodes by curing-induced compression stress. Electrochimica Acta 100 (2013) 85-92 https://doi.org/10.1016/j.electacta.2013.03.127
[23] H. Kim; T. Hwang. Effect of titanium isopropoxide addition in low-temperature cured TiO 2 photoanode for a flexible DSSC. Journal of sol-gel science and technology 72 (2014) 67-73 https://doi.org/10.1007/s10971-014-3427-0
[24] A. Sclafani; M.-N. Mozzanega; P. Pichat. Effect of silver deposits on the photocatalytic activity of titanium dioxide samples for the dehydrogenation or oxidation of 2-propanol. Journal of Photochemistry and Photobiology A: Chemistry 59 (1991) 181-189 https://doi.org/10.1016/1010-6030(91)87006-H
[25] S.Y.T. Camacho; A. Rey; M.D. Hernández-Alonso; J. Llorca; F. Medina; S. Contreras. Pd/TiO2-WO3 photocatalysts for hydrogen generation from water-methanol mixtures. Applied Surface Science 455 (2018) 570-580 https://doi.org/10.1016/j.apsusc.2018.05.122
[26] D. Wodka; E. Bielanska; R.P. Socha; M. Elzbieciak-Wodka; J. Gurgul; P. Nowak; P. Warszyński; I. Kumakiri. Photocatalytic activity of titanium dioxide modified by silver nanoparticles. ACS applied materials & interfaces 2 (2010) 1945-1953 https://doi.org/10.1021/am1002684
[27] C.-C. Wang; J.Y. Ying. Sol-gel synthesis and hydrothermal processing of anatase and rutile titania nanocrystals. Chemistry of Materials 11 (1999) 3113-3120 https://doi.org/10.1021/cm990180f
[28] Z. Zhang; C.-C. Wang; R. Zakaria; J.Y. Ying. Role of particle size in nanocrystalline TiO2-based photocatalysts. The Journal of Physical Chemistry B 102 (1998) 10871-10878 https://doi.org/10.1021/jp982948
[29] T. McMurray; J. Byrne; P. Dunlop; J. Winkelman; B. Eggins; E. McAdams. Intrinsic kinetics of photocatalytic oxidation of formic and oxalic acid on immobilised TiO2 films. Applied Catalysis A: General 262 (2004) 105-110 https://doi.org/10.1016/j.apcata.2003.11.013
[30] J. Krýsa; G. Waldner; H. Měšťánková; J. Jirkovský; G. Grabner. Photocatalytic degradation of model organic pollutants on an immobilized particulate TiO2 layer: Roles of adsorption processes and mechanistic complexity. Applied Catalysis B: Environmental 64 (2006) 290-301 https://doi.org/10.1016/j.apcatb.2005.11.007
[31] T. Tatsuma; K. Suzuki. Photoelectrochromic cell with a Ag–TiO2 nanocomposite: concepts of drawing and display modes. Electrochemistry Communications 9 (2007) 574-576. https://doi.org/10.1016/j.elecom.2006.10.044
[32] K. Naoi; Y. Ohko; T. Tatsuma. TiO2 films loaded with silver nanoparticles: control of multicolor photochromic behavior. Journal of the American Chemical Society 126 (2004) 3664-3668 https://doi.org/10.1021/ja039474z
[33] I. Tanabe; T. Tatsuma. Plasmonic manipulation of color and morphology of single silver nanospheres. Nano letters 12 (2012) 5418-5421 https://doi.org/10.1021/nl302919n
[34] K. Matsubara; T. Tatsuma. Morphological changes and multicolor photochromism of Ag nanoparticles deposited on single-crystalline TiO2 surfaces. Advanced Materials 19 (2007) 2802-2806 https://doi.org/10.1002/adma.200602823
[35] N. Sobana; K. Selvam; M. Swaminathan. Optimization of photocatalytic degradation conditions of Direct Red 23 using nano-Ag doped TiO2. Separation and Purification Technology 62 (2008) 648-653 https://doi.org/10.1016/j.seppur.2008.03.002
[36] D. Shchukin; E. Ustinovich; D. Sviridov; P. Pichat. Effect of silver deposits on the photocatalytic activity of titanium dioxide for the removal of 2-chlorophenol in water. Photochemical & Photobiological Sciences 3 (2004) 142-144 https://doi.org/10.1039/b306077b
[37] M. Shokri; A. Jodat; N. Modirshahla; M.A. Behnajady. Photocatalytic degradation of chloramphenicol in an aqueous suspension of silver-doped TiO2 nanoparticles. Environmental technology 34 (2013) 1161-1166 https://doi.org/10.1080/09593330.2012.743589
[38] T. Sano; N. Negishi; D. Mas; K. Takeuchi. Photocatalytic decomposition of N2O on highly dispersed Ag+ ions on TiO2 prepared by photodeposition. Journal of Catalysis 194 (2000) 71-79 https://doi.org/10.1006/jcat.2000.2915